Coexisting Néel and charge density wave orders in attractive three-color fermions

Xiang Li and Yu Wang*
School of Physics and Technology, Wuhan University, Wuhan 430072, China

(Received 7 May 2024; revised 25 July 2024; accepted 18 August 2024; published 3 September 2024)

In optical lattices attractive ultracold fermions with three hyperfine-spin components (colors) can form three fermionic configurations depending on the interactions—unbound fermions, on-site trions, and off-site trions—leading to the coexistence of multiple fermionic species in the ordered phase, which demonstrates that the attractive three-color fermions are unique from other correlated fermion systems and may host intriguing phases and phase transitions. At temperatures below the superexchange energy scale, we employ the determinant quantum Monte Carlo (QMC) method to investigate the phases and phase transitions in the half-filled attractive three-color Hubbard model on a honeycomb lattice where the Hubbard interactions are color dependent (anisotropic interactions) and the coupling between color 3 and colors (1, 2) serves as a control parameter. In the coupling regime where on-site and off-site trions coexist, our QMC simulations demonstrate coexisting Néel and charge density wave (CDW) orders which are common in condensed matter but rare in ultracold atoms. At weak coupling where the color superfluid (CSF) order is scattered by color-3 fermions, we find that very small coupling of color 3 with colors (1, 2) can destroy the CSF order and that the vanishing of the CSF order is not immediately accompanied by the emergence of the on-site trionic phase, which strikingly disagrees with the prevalent results of dynamical mean-field theory. The underlying mechanisms of the coexisting Néel/CDW orders and of the CSF order breaking are also presented based on intuitive physical pictures.

DOI: 10.1103/PhysRevB.110.115105

I. INTRODUCTION

SU(3) physics with attractive three-color (hyperfine-spin component) ultracold fermions, such as ^{6}Li and ^{40}K atoms [1–3], is one of the major research centers of interest at the interdisciplinary frontiers of ultracold atom physics, condensed-matter physics, and high-energy physics. The attractive SU(3) Fermi gas with a tunable interaction is an ideal system for studying trimer states which are hard to be realized in spin-1/2 Fermi gas due to the Pauli exclusion [4–6]. In optical lattices loaded with attractive SU(3) ultracold fermions, the variational [7,8], self-energy functional [9,10], dynamical mean-field theory (DMFT) [11,12], and Bethe ansatz [13] studies have demonstrated the phase transition between the color superfluid (CSF) phase and the on-site trionic phase. This is strongly reminiscent of the phase transition between the quark superfluid state and the baryon state in high-energy physics [14–16]. Moreover, DMFT studies [17,18] have also shown a direct phase transition between the CSF phase and the on-site trionic phase in the attractive three-color Hubbard model where attractions are color dependent, thus breaking the SU(3) symmetry of the Hamiltonian. Besides the on-site trion, more interestingly, the exact diagonalization study of the three-fermion attractive SU(3) Hubbard model on the honeycomb lattice suggests another type of three-body bound state, known as the off-site trion, composed of two fermions at one site and one fermion at the nearest-neighbor site [19].

In recent years, the long-ignored role of the off-site trions in many-body physics of attractive three-color fermions has been considered. In a one-dimensional lattice away from half filling, the density matrix renormalization group studies have shown that off-site trions can develop quasi-long-range correlations in the attractive SU(3) Hubbard model with suppressed on-site triple occupancy [20] as well as in the attractive three-color Hubbard model with significantly anisotropic interactions [21]. Recently, quantum Monte Carlo (QMC) simulations of the half-filled attractive SU(3) Hubbard model on a honeycomb lattice have shown that on-site trions (majority) and off-site trions (minority) coexist in the charge density wave (CDW) state [22,23], and the off-site trion arising from density fluctuations forms a local bond state [22]. Unlike conventional transitions in which only a single fermionic species gets involved, off-site trions, though small in number, together with on-site trions, participate in the CDW ordering of the attractive SU(3) Dirac fermions, and particularly the quantum critical point affected by multiple fermionic species cannot be described using the conventional Gross-Neveu-Yukawa paradigm [22].

In this paper, we explore quantum phase transitions in the half-filled attractive three-color Hubbard model on a honeycomb lattice. The coupling between the third color and the other two colors serves as a control parameter of phase transitions. On one hand, breaking SU(3) symmetry results in "magnetic" off-site trions (two ends of which may carry net colors), and on the other hand, reducing the coupling of the third color with the other two colors (namely, introducing "interaction anisotropy") enhances the density fluctuations, which in turn lead to an increase in the number of off-site

*Contact author: yu.wang@whu.edu.cn

 ©2024 American Physical Society

trions. Thus the magnetic ordering of the off-site trions may develop in the attractive three-color Hubbard model. Our sign-problem-free QMC simulations demonstrate coexisting Néel and CDW orders via tuning the interaction anisotropy in attractive three-color fermionic atoms, while the previously reported coexistence of charge and magnetic orders that usually occurs in condensed matter [24–42] is rare in ultracold atoms. In addition, our QMC results disagree with the DMFT prediction that a direct phase transition between the CSF order and the on-site trionic order may occur in the half-filled attractive three-color Hubbard model.

The rest of this paper is organized as follows. In Sec. II, the model Hamiltonian and parameters of QMC simulations are introduced. The coexisting Néel and CDW orders are then studied in Sec. III. Subsequently, in Sec. IV, the mechanism of CSF order breaking is investigated. Thereafter, Sec. V presents the phase diagram of the model calculated by QMC simulations. The conclusions are drawn in Sec. VI.

II. MODEL AND METHOD

The half-filled attractive three-color Hubbard model on the honeycomb lattice is described by the following Hamiltonian,

$$H = -t\sum_{\langle ij\rangle,\alpha}(c^{\dagger}_{i\alpha}c_{j\alpha}+\text{H.c.}) + \sum_{i,\alpha<\beta}U_{\alpha\beta}\left(n_{i\alpha}-\frac{1}{2}\right)\left(n_{i\beta}-\frac{1}{2}\right), \tag{1}$$

where $\langle ij\rangle$ denotes a pair of nearest-neighbor sites; α and β are the color indices taking only values $1, 2, 3$; t is the nearest-neighbor hopping integral; $n_{i\alpha}=c^{\dagger}_{i\alpha}c_{i\alpha}$ is the particle number operator of color α on site i; $U_{\alpha\beta}(<0)$ is the attractive interaction between fermions carrying different colors. The chemical potential vanishes at half filling. Inspired by the theoretical and experimental works regarding the SU(N)-symmetry breaking interactions [43–46], we set $U_{12}=U$ and $U_{13}=U_{23}=U'$ throughout the paper. Note that $|U'|/|U|$ characterizes the interaction anisotropy. When $|U|=|U'|$, the interaction is color independent (isotropic) and the Hamiltonian Eq. (1) possesses SU(3) symmetry; when $|U'|<|U|$, the interaction anisotropy is introduced and the SU(3) symmetry of the Hamiltonian Eq. (1) is reduced to SU(2) $\otimes$ U(1); when $U'=0$, the system is decoupled into two subsystems, namely SU(2) interacting fermions and free fermions, owning SO(4) $\otimes$ U(1) symmetry [47].

The determinant QMC simulation of the half-filled attractive three-color Hubbard model is sign-problem-free when the Hubbard-Stratonovich decomposition in the spin-flip channel is employed [22,23,48]. We employ the determinant QMC method at $T=0.1t$ (below the superexchange energy scale) to simulate the phase transitions in the attractive three-color Hubbard model. The simulations are performed on the finite-sized honeycomb lattices with the linear lattice sizes [49] $L=3, 6, 9, 12$, in which case the total number of lattice sites is $2L^2$. Unless specifically stated, the color-dependent Hubbard interactions $U_{\alpha\beta}$ are given in the units of t.

III. COEXISTING NÉEL/CDW ORDERS

To gain some insight into the physics of the half-filled attractive three-color Hubbard model, we first consider the two-site model. For infinite coupling, an on-site trion forms. In the strong-coupling limit, the perturbation theory gives the first-order correction term which is cast in the form of an off-site trion,

$$|\psi_{\text{off}}\rangle = -\frac{t}{|U|+|U'|}(|12,3\rangle+|13,2\rangle+|23,1\rangle) + \left(-\frac{t}{2|U'|}+\frac{t}{|U|+|U'|}\right)|12,3\rangle. \tag{2}$$

We see that the off-site trion takes a Néel-like configuration due to the second term on the right-hand side of Eq. (2) [the first term is SU(3) symmetric and "colorless"], when interactions become anisotropic, $|U'|<|U|$.

In the trionic CDW regime where on-site and off-site trions coexist, density fluctuations lead to the formation of off-site trions from on-site trions [22,23]. Interaction anisotropy $|U'|<|U|$ enhances density fluctuations, thus driving up the number of off-site trions. Our determinant QMC simulations demonstrate that interaction anisotropy can induce the Néel ordering of off-site trions on the background of the trionic CDW phase. In this section, we set $|U|=6$ in order to broaden the coupling range of $|U'|$ ($<|U|$) in which on-site and off-site trions coexist [22].

The structures of trions can be described, respectively, by the on-site triple occupancy

$$P_3=\frac{1}{N}\sum_i\langle n_{i1}n_{i2}n_{i3}\rangle, \tag{3}$$

and the off-site triple occupancies

$$P_{3\text{off};1}=\frac{1}{3N}\sum_{\langle ij\rangle}\langle n_{i2}n_{i3}n_{j1}\rangle, \qquad P_{3\text{off};3}=\frac{1}{3N}\sum_{\langle ij\rangle}\langle n_{i1}n_{i2}n_{j3}\rangle, \tag{4}$$

where N is the number of lattice sites. The dependences of occupancies P_3, $P_{3\text{off};1}$, and $P_{3\text{off};3}$ on the coupling strength $|U'|$ are presented in Fig. 1. In the whole range of $3\leqslant|U'|\leqslant 6$, $P_3\gg P_{3\text{off}}>0$, which shows that the minority off-site trions coexist with the majority on-site trions. Evidently, when $|U'|<5.5$, $P_{3\text{off};3}>P_{3\text{off};1}$, which implies that color 3 and colors (1, 2) carried by off-site trions tend to occupy different sublattices (i.e., forming Néel-like off-site trions). The QMC results agree with our physical intuition coming from the first-order perturbation theory of the two-site Hubbard model. Moreover, with the decrease of $|U'|$, $P_{3\text{off}}$ increases while P_3 decreases, which displays the physical picture that interaction-anisotropy enhanced density fluctuations promote the formation of off-site trions from on-site trions.

We next show that the growing number of Néel-like off-site trions caused by the interaction anisotropy can develop Néel order. The Néel configuration in our three-color model is contributed by the net magnetic moments of the off-site trion: The two-fermion end with net colors (1, 2) is in sublattice A, while the one-fermion end with net color 3 is in sublattice B.

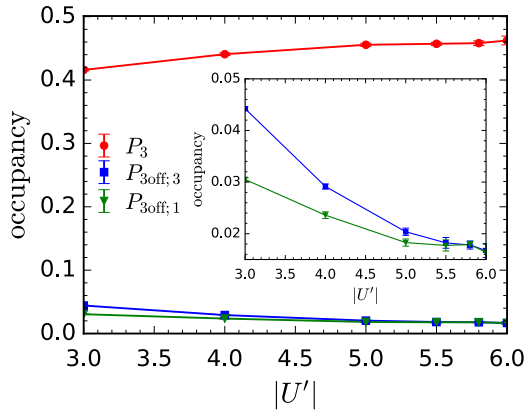

FIG. 1. The on-site triple occupancy P_3, and off-site triple occupancies $P_{3\text{off};1}$ and $P_{3\text{off};3}$ are plotted as functions of $|U'|$. The inset is a zoom-in view of $P_{3\text{off};1}$ and $P_{3\text{off};3}$ curves. The lattice size is $L = 9$.

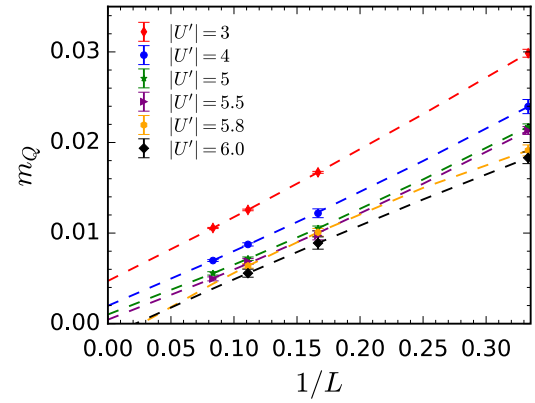

FIG. 2. The finite-size extrapolation of the Néel order parameter m_Q for various $|U'|$. The quadratic polynomial fitting is used.

As explained in the Appendix, the Néel moment operator on site i can be defined as

$$m_i = \tfrac{1}{4}(n_{i1} + n_{i2} - 2n_{i3}), \tag{5}$$

which yields the Néel moment $\langle m_i \rangle = (-1)^i \frac{1}{2}$. The Néel order parameter is then defined as a sum over the correlations between Néel moment operators,

$$m_Q = \frac{1}{N}\sqrt{\sum_{ij}(-1)^{i+j}\langle m_i m_j\rangle}. \tag{6}$$

To investigate the charge spatial modulation (CSM), we also calculate the staggered order parameters [50–53]

$$\begin{aligned} M_1 &= \frac{1}{N}\sqrt{\sum_{ij}(-1)^{i+j}\langle n_{i1}n_{j1}\rangle}, \\ M_3 &= \frac{1}{N}\sqrt{\sum_{ij}(-1)^{i+j}\langle n_{i3}n_{j3}\rangle}, \end{aligned} \tag{7}$$

and the trionic CDW order parameter [22,23]

$$D = \frac{1}{N}\sqrt{\sum_{i,j}(-1)^{i+j}C(i,j)}, \tag{8}$$

where $C(i,j) = \sum_{\alpha,\beta}\langle n_{i\alpha}n_{j\beta}\rangle$ is the density-density correlation function. For various couplings in the range $3 \leqslant |U'| \leqslant 6$, the Néel order parameter m_Q, the trionic CDW order parameter D, and the staggered order parameters M_1 and M_3 are obtained by a finite-size extrapolation of the QMC data, as shown in Figs. 2 and 3, respectively.

Based on the finite-size extrapolation result for the order parameters, the Néel order parameter m_Q, the trionic CDW order parameter D, and the staggered order parameters M_1 and M_3 are respectively plotted as functions of $|U'|$ in Fig. 4. As shown in Fig. 4(a), when the coupling strength $|U'| < 5.5$, Néel ordering develops ($m_Q > 0$). In Fig. 4(b), on one hand, in the specified coupling regime the trionic CDW order parameter D is slightly smaller than its limiting value, 1.5 (in this limit only on-site trions exist and they occupy one sublattice), indicating that the strong trionic CDW order develops in the mixture of on-site trions and off-site trions; on the other hand,

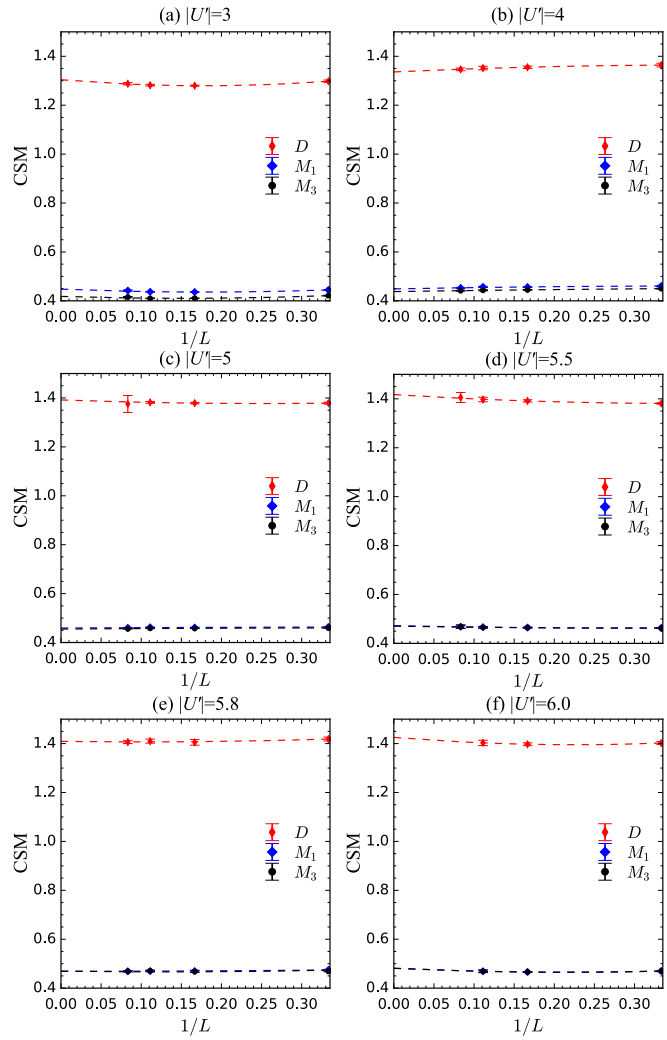

FIG. 3. The finite-size extrapolation of the trionic CDW order parameter D and staggered order parameters M_1 and M_3 at (a) $|U'| = 3$, (b) $|U'| = 4$, (c) $|U'| = 5$, (d) $|U'| = 5.5$, (e) $|U'| = 5.8$, and (f) $|U'| = 6$. Order parameters D, M_1, and M_3 characterize the charge spatial modulation (CSM) of three-color fermions. The quadratic polynomial fitting is used.

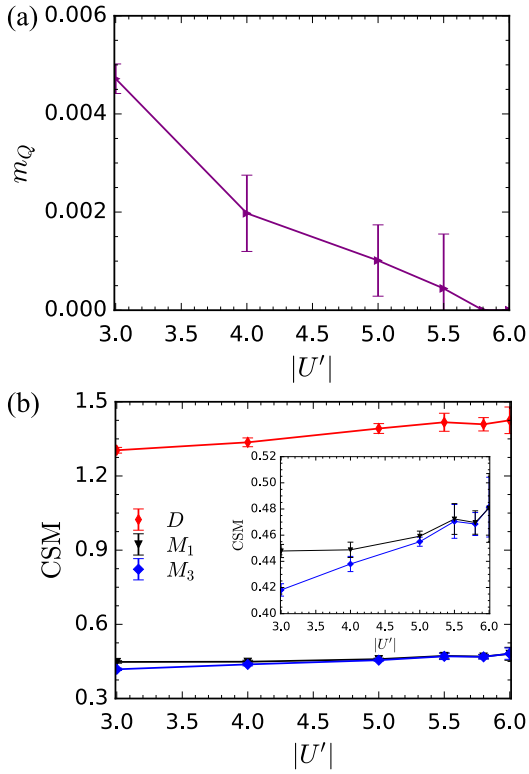

FIG. 4. (a) The plot of the Néel order parameter m_Q as a function of $|U'|$. (b) The plots of the trionic CDW order parameter D and the staggered order parameters M_1 and M_3 as functions of $|U'|$. The inset is a zoom-in view of M_1 and M_3 curves.

when $|U'| < 5.5$, staggered order parameters obey $M_3 < M_1$, which indicates that on the background of the trionic CDW order, the one-fermion ends of off-site trions carrying net color 3 tend to be the nearest neighbors of on-site trions and thus occupy a sublattice [two-fermion ends of the off-site trions carrying net colors (1, 2) then occupy the other sublattice], reflecting the Néel ordering of off-site trions. When $|U'| \geqslant 5.5$, M_1 and M_3 curves coincide perfectly with each other [Fig. 4(b)], demonstrating the vanishing of the Néel-like configuration of an off-site trion, and accordingly Néel order $m_Q = 0$ [Fig. 4(a)]. Our QMC results clearly show that the control of coupling strength $|U'|$ induces the Néel ordering of off-site trions on the background of the strong trionic CDW order.

We can intuitively comprehend, on the energy grounds, the underlying physics of Néel ordering of the off-site trions. On the background of the trionic CDW order, an off-site trion only has two possible orientations: (1) Its one-fermion end is the nearest neighbor to on-site trions, as illustrated in Fig. 5(a), and (2) its two-fermion end is the nearest neighbor to on-site trions, as depicted in Fig. 5(b). The Pauli exclusion blocks more hopping channels in Fig. 5(b) than in Fig. 5(a). Hence, to lower the total kinetic energy, Néel-like off-site trions [resulting from breaking SU(3) symmetry of Hubbard interactions] tend to follow the spatial arrangement outlined in Fig. 5(a), which is exactly the same as QMC results. Since the two ends of Néel-like off-site trions occupy a different sublattice, the Néel ordering develops when the number of off-site trions

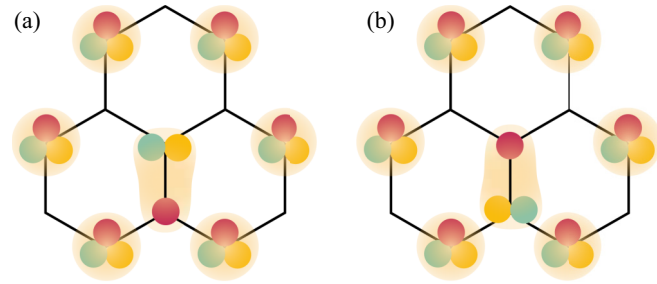

FIG. 5. Two possible orientations of an off-site trion on the background of the trionic CDW order: (a) The one-fermion end of the off-site trion is the nearest neighbor to on-site trions. (b) The two-fermion end of the off-site trion is the nearest neighbor to on-site trions.

continues to increase due to the enhanced density fluctuation via tuning the coupling of color 3 with colors (1, 2) $|U'|$.

In the half-filled attractive SU(3) Hubbard model, increasing the color-independent Hubbard interaction induces only the CDW order that corresponds to the spatial modulation of both on-site and off-site trions on a bipartite lattice [22,23]. Breaking the SU(3) symmetry of the Hubbard interaction not only causes the off-site trions to be Néel-like, but also enhances the density fluctuations promoting the formation of off-site trions from on-site trions. As a consequence, Néel ordering of the ever-increasing Néel-like off-site trions occurs on the background of the on-site trionic CDW order. Therefore, the color-dependent Hubbard interactions (i.e., interaction anisotropy) play a key role in developing the coexisting Néel and CDW orders.

IV. CSF ORDER BREAKING

When the color-3 fermion is weakly coupled to the CSF state of fermions carrying colors (1, 2) (i.e., $|U'| \ll |U|$), DMFT studies [17,18] suggest a direct phase transition between the CSF state and the on-site trionic state at finite $|U'|$. We argue that CSF order vanishes at very small $|U'|$ accompanied by the symmetry reduction from SO(4) ⊗ U(1) to SU(2) ⊗ U(1), and the on-site trionic phase does not emerge immediately after breaking the CSF order since $|U'|$ is very small. Our point can be verified by QMC simulations.

We first define the s-wave pairing (i.e., CSF) structure factor

$$\Delta_s = \frac{1}{N}\sum_{ij}\langle c_{i1}^\dagger c_{i2}^\dagger c_{j2} c_{j1} + \text{H.c.}\rangle. \tag{9}$$

The CSF order parameter is then expressed as $\Delta = \sqrt{\Delta_s/N}$. To characterize the densities of pairs and on-site trions, we also calculate the double occupancy

$$P_2 = \frac{1}{N}\sum_i \langle n_{i1} n_{i2}\rangle, \tag{10}$$

and the triple occupancy P_3 for various small $|U'|$ around the SO(4) ⊗ U(1) symmetric point. In this section, the coupling between colors 1 and 2 is set to $|U| = 6$. As shown in Fig. 6, the square of CSF order parameter Δ^2 for various small couplings ($|U'| \leqslant 0.175$) are obtained by a finite-size

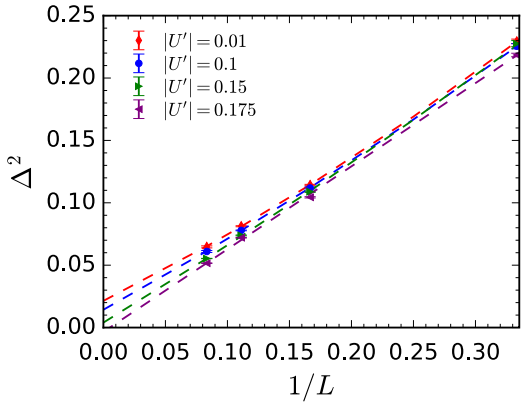

FIG. 6. The finite-size extrapolation of the square of CSF order parameter Δ^2 for various $|U'|$. The quadratic polynomial fitting is used.

extrapolation. In Fig. 7, the square of the CSF order parameter Δ^2, the double occupancy P_2, and the triple occupancy P_3 are plotted as functions of the coupling strength $|U'|$. When the coupling $|U'| \geqslant 0.175$, the CSF order vanishes while the double occupancy P_2 is almost unchanged near the transition point and is still much larger than the triple occupancy P_3 (which is almost unchanged as well). This evidently suggests that the dominant entities are pairs rather than on-site trions immediately after the vanishing of the CSF order, which disagrees with the DMFT results [17,18].

The mechanism of vanishing CSF order around the SO(4) ⊗ U(1) symmetric point can be intuitively understood in the two-site model by virtue of the concept of Bose-Einstein condensate (BEC) of pairs [49,54]. In the subsystem of fermions carrying colors (1, 2), at strong attractive couplings, pairs develop into the phase coherent BEC state

$$|\psi\rangle = e^{e^{i\phi}\sum_i c_{i1}^\dagger c_{i2}^\dagger}|0\rangle, \tag{11}$$

in which the average of the pairing structure factor is $\langle\psi|\Delta_s|\psi\rangle = 4$. However, when a pair carrying colors (1, 2) is scattered by a color-3 fermion on a site, as is illustrated in Fig. 8(a), the phase on the scattering site is shifted, resulting in that the BEC of pairs evolves into a phase incoherent state

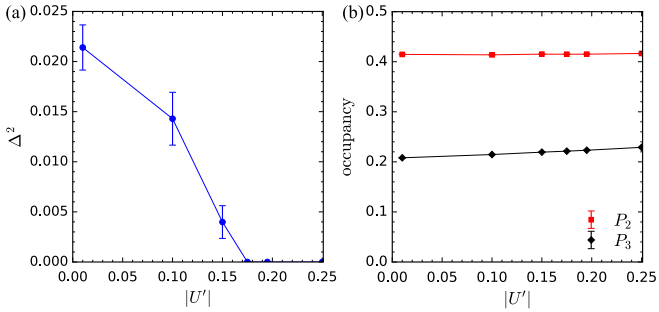

FIG. 7. (a) The square of CSF order parameter Δ^2, and (b) the double occupancy P_2 and the triple occupancy P_3 are plotted as functions of the coupling strength $|U'|$. P_2 and P_3 are calculated on the $L = 9$ lattice. Error bars are smaller than the data points in (b).

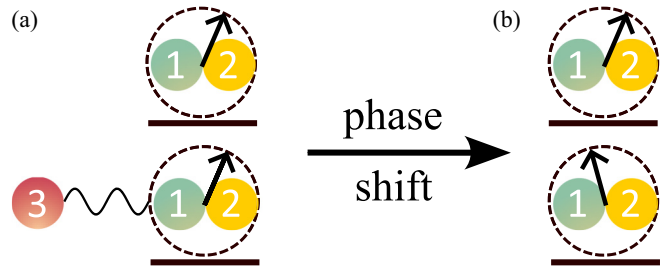

FIG. 8. (a) The phase coherent pairs carrying colors (1, 2) are scattered by the color-3 fermions, (b) leading to incoherent doublons.

(doublons)

$$|\psi'\rangle = e^{(e^{i\phi}c_{11}^\dagger c_{12}^\dagger + e^{i(\phi+\Delta\phi)}c_{21}^\dagger c_{22}^\dagger)}|0\rangle, \tag{12}$$

as is illustrated in Fig. 8(b). In the phase incoherent state, the pairing structure factor decreases since $\langle\psi'|\Delta_s|\psi'\rangle = 2 + 2\cos(\Delta\phi) < 4$. This microscopic picture of the CSF-breaking mechanism illustrates that, before the development of the trionic phase, the CSF order vanishes along with the emergence of incoherent doublons, because the phase shift caused by the color-3 fermion scattering destroys the phase coherence in the BEC of pairs, leading to suppression of the pairing correlation.

V. PHASE DIAGRAM

At $T = 0.1$, the phase diagram of the half-filled attractive three-color Hubbard model is shown in Fig. 9. Here, the interaction anisotropy $|U'|/|U|$ and the coupling between colors 1 and 2 serve as control parameters for phase transitions. All data points (order parameters) are obtained by the finite-size extrapolation of the order parameters (calculated on the $L = 3, 6, 9$ honeycomb lattices) to their $L \to \infty$ limits. Note that the black legends in the phase diagram represent sufficiently weak order parameters that can be identified by our QMC simulations. The white star represents the vanishing Néel order parameter, while the black star denotes the weak Néel order. The midpoints between the corresponding black and white stars depict the phase boundary separating the

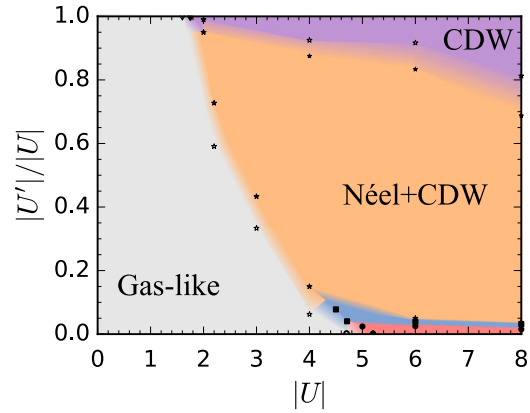

FIG. 9. The phase diagram of the half-filled attractive three-color Hubbard model on the honeycomb lattice at $T = 0.1$. The blue and red regions are the doublon-CDW phase and the coexisting doublon-CDW/CSF phases, respectively.

coexisting Néel/CDW phases from the gaslike and CDW phases. The (topmost) black and white inverted triangles represent respectively the weak and vanishing CDW orders. The black square and circle represent respectively the weak doublon-CDW and CSF orders. In the regime of small $|U'|/|U|$, the black squares enclose the region of the doublon-CDW phase in which the black circles indicate the subarea of the coexisting doublon-CDW/CSF phases [near the SO(4) $\otimes$ U(1) symmetric point]. The (downmost) white circle represents the vanishing CSF order.

The phase diagram consists of five regions that represent the different phases marked by color. In the gaslike phase (gray region), the spatial distributions of fermions and their color indices are uniform, described by the vanishing staggered order parameters $M_1 = M_3 = 0$. In the trionic CDW phase (purple region), the CDW order parameter $D > 0$, while the Néel order parameter $m_Q = 0$ and the staggered order parameters $M_1 = M_3 > 0$ [since this region is near the SU(3) symmetric point]. In the coexisting Néel/CDW phase (yellow region), the order parameters satisfy the conditions $D > 0, m_Q > 0$, and $M_1 > M_3 > 0$ [away from the SU(3) symmetric point]. In the doublon-CDW phase (blue region), staggered order parameters $M_1 > 0$ and $M_3 = 0$, in which case, fermions with colors 1 and 2 form the doublon-CDW phase while the distribution of color-3 fermions is spatially uniform. In the coexisting doublon-CDW/CSF phase (red region), the staggered order parameters $M_1 > 0$ and $M_3 = 0$, and the CSF order parameter $\Delta > 0$. The phase diagram of our model clearly shows that the Néel and CDW orders coexist over a broad range of parameters, and that the CSF and trionic CDW phases are separated by a narrow strip of the doublon-CDW phase.

VI. CONCLUSIONS

We have performed the sign-problem-free determinant QMC simulations at $T = 0.1$ to investigate the phase transitions in the half-filled attractive three-color Hubbard model on a honeycomb lattice, where Hubbard interactions are color dependent and set as $|U_{1,2}| = |U| = 6$ and $|U_{1,3}| = |U_{2,3}| = |U'|$. The coupling $|U'|$ serves as a control parameter inducing phase transitions. In the coupling regime $3 \leqslant |U'| \leqslant 6$ where on-site and off-site trions coexist, our QMC simulations demonstrate the coexisting Néel and CDW orders driven by interaction anisotropy $|U'| < |U|$. The Néel order is developed by the Néel-like off-site trions, while the CDW order is modulated by both on-site and off-site trions. In the weak-coupling regime $|U'| < 0.25$, our QMC result shows that double-occupancy probability is almost $|U'|$ independent and much greater than the triple-occupancy probability, which implies that the vanishing of the CSF order is not immediately accompanied by the emergence of the on-site trionic phase.

The coexistence of spin/charge orders has long been a research focus in condensed-matter physics, but yet absent in cold atom physics. In the phase diagram calculated by our QMC simulations, the coexisting Néel and CDW orders occur over a wide range of the control parameters when the half-filled attractive three-color Hubbard model is away from the SU(3) and SO(4) $\otimes$ U(1) symmetric points. The system of attractive three-color fermions can accommodate multiple fermionic species (unbound single fermion, on-site trion, and off-site trion) along with the variation of couplings, which makes it unique from other correlated fermionic systems. Our work opens up an avenue for exploring many-body physics of attractive three-color fermions depending on the interplay of three fermionic species, which may host intriguing quantum phases and phase transitions.

ACKNOWLEDGMENTS

This work is financially supported by the National Natural Science Foundation of China under Grants No. 11874292, No. 11729402, and No. 11574238. We gratefully acknowledge Lev Kantorovich for a critical reading of the manuscript. We acknowledge the support of the Supercomputing Center of Wuhan University.

APPENDIX: DEFINITION OF NÉEL ORDER

In the SU(N) Hubbard model, the two-point spin-spin correlation function should be defined as

$$S_{\text{spin}}(i, j) = \sum_n \langle S^n(i) S^n(j) \rangle, \tag{A1}$$

where $S^n(i)$ is the nth SU(N) generator on site i [55–58]. For the SU(3) case, $S^n(i)$ takes the form of $c^\dagger_{i\alpha} \hat{\lambda}^n_{\alpha\beta} c_{i\beta}$, in which $\hat{\lambda}^n$ is the nth Gell-Mann matrix [59]. However, in the SU(N)-symmetry-breaking Hubbard model, generators make unequal contributions to the spin-spin correlation function defined by Eq. (A1), and usually, only generators with major contributions are retained when testing magnetic order. For instance, in the SU(2)-symmetry-breaking Hubbard model, only $S^z(i)$ is included in the spin-spin correlation function [60]; in the SU($2N$)-symmetry-breaking Hubbard model, only diagonal generators are included in the spin-spin correlation function [61]. In the attractive three-color Hubbard model, since magnetism arises from the net magnetic moments of the off-site trions [the two-fermion end carries net colors (1,2) while the one-fermion end carries net color 3], the eighth SU(3) generator $S^8(i)$,

$$(c^\dagger_{i1}, c^\dagger_{i2}, c^\dagger_{i3}) \frac{1}{\sqrt{3}} \begin{pmatrix} 1 & 0 & 0 \\ 0 & 1 & 0 \\ 0 & 0 & -2 \end{pmatrix} \begin{pmatrix} c_{i1} \\ c_{i2} \\ c_{i3} \end{pmatrix}, \tag{A2}$$

makes a much larger contribution to the spin-spin correlation function than other SU(3) generators. Thus we can only retain $S^8(i)$ in the spin-spin correlation function when testing the Néel order. Parallel to Ref. [62], in which the magnetic order is defined in terms of the spatial arrangement of magnetic moments, we define for the SU(3)-symmetry-breaking model the Néel order parameter as

$$m_Q = a \frac{1}{N} \sqrt{\sum_{ij} (-1)^{i+j} \langle S^8(i) S^8(j) \rangle}, \tag{A3}$$

where a is a coefficient.

[1] T. B. Ottenstein, T. Lompe, M. Kohnen, A. N. Wenz, and S. Jochim, Collisional stability of a three-component degenerate Fermi gas, Phys. Rev. Lett. **101**, 203202 (2008).

[2] J. H. Huckans, J. R. Williams, E. L. Hazlett, R. W. Stites, and K. M. O'Hara, Three-body recombination in a three-state Fermi gas with widely tunable interactions, Phys. Rev. Lett. **102**, 165302 (2009).

[3] C. A. Regal and D. S. Jin, Measurement of positive and negative scattering lengths in a Fermi gas of atoms, Phys. Rev. Lett. **90**, 230404 (2003).

[4] D. Mattis and S. Rudin, Three-body bound states on a lattice, Phys. Rev. Lett. **52**, 755 (1984).

[5] S. Rudin, Absence of binding of three fermions on a two-dimensional lattice, Phys. Rev. A **31**, 3441 (1985).

[6] D. C. Mattis, The few-body problem on a lattice, Rev. Mod. Phys. **58**, 361 (1986).

[7] A. Rapp, G. Zaránd, C. Honerkamp, and W. Hofstetter, Color superfluidity and "baryon" formation in ultracold fermions, Phys. Rev. Lett. **98**, 160405 (2007).

[8] A. Rapp, W. Hofstetter, and G. Zaránd, Trionic phase of ultracold fermions in an optical lattice: A variational study, Phys. Rev. B **77**, 144520 (2008).

[9] K. Inaba and S.-I. Suga, Finite-temperature properties of attractive three-component fermionic atoms in optical lattices, Phys. Rev. A **80**, 041602(R) (2009).

[10] K. Inaba and S.-i. Suga, Color superfluid and trionic state of attractive three-component lattice fermionic atoms at finite temperatures, Mod. Phys. Lett. B **25**, 987 (2011).

[11] I. Titvinidze, A. Privitera, S.-Y. Chang, S. Diehl, M. A. Baranov, A. Daley, and W. Hofstetter, Magnetism and domain formation in SU(3)-symmetric multi-species Fermi mixtures, New J. Phys. **13**, 035013 (2011).

[12] A. Koga and H. Yanatori, Spontaneously symmetry-breaking states in the attractive SU(N) Hubbard model, J. Phys. Soc. Jpn. **86**, 034702 (2017).

[13] W. J. Chetcuti, J. Polo, A. Osterloh, P. Castorina, and L. Amico, Probe for bound states of SU(3) fermions and colour deconfinement, Commun. Phys. **6**, 128 (2023).

[14] Z. Fodor and S. D. Katz, Lattice determination of the critical point of QCD at finite T and μ, J. High Energy Phys. 03 (2002) 014.

[15] Y. Aoki, G. Endrődi, Z. Fodor, S. D. Katz, and K. K. Szabo, The order of the quantum chromodynamics transition predicted by the standard model of particle physics, Nature (London) **443**, 675 (2006).

[16] F. Wilczek, Lifestyles of the small and simple, Nat. Phys. **3**, 375 (2007).

[17] Y. Okanami, N. Takemori, and A. Koga, Stability of the superfluid state in three-component fermionic optical lattice systems, Phys. Rev. A **89**, 053622 (2014).

[18] S. Miyatake, K. Inaba, and S. Suga, Color superfluidity and trionic state of three-component lattice fermionic atoms, J. Phys.: Conf. Ser. **273**, 012008 (2011).

[19] J. Pohlmann, A. Privitera, I. Titvinidze, and W. Hofstetter, Trion and dimer formation in three-color fermions, Phys. Rev. A **87**, 023617 (2013).

[20] A. Kantian, M. Dalmonte, S. Diehl, W. Hofstetter, P. Zoller, and A. J. Daley, Atomic color superfluid via three-body loss, Phys. Rev. Lett. **103**, 240401 (2009).

[21] P. Azaria, S. Capponi, and P. Lecheminant, Three-component Fermi gas in a one-dimensional optical lattice, Phys. Rev. A **80**, 041604(R) (2009).

[22] H. Xu, X. Li, Z. Zhou, X. Wang, L. Wang, C. Wu, and Y. Wang, Trion states and quantum criticality of attractive SU(3) Dirac fermions, Phys. Rev. Res. **5**, 023180 (2023).

[23] X. Li, H. Xu, and Y. Wang, Quantum Monte Carlo simulations of thermodynamic properties of attractive SU(3) Dirac fermions, Phys. Rev. B **108**, 165102 (2023).

[24] Y. Zhang, E. Demler, and S. Sachdev, Competing orders in a magnetic field: Spin and charge order in the cuprate superconductors, Phys. Rev. B **66**, 094501 (2002).

[25] S. A. Kivelson, I. P. Bindloss, E. Fradkin, V. Oganesyan, J. M. Tranquada, A. Kapitulnik, and C. Howald, How to detect fluctuating stripes in the high-temperature superconductors, Rev. Mod. Phys. **75**, 1201 (2003).

[26] A. V. Balatsky, D. N. Basov, and J.-X. Zhu, Induction of charge density waves by spin density waves in iron-based superconductors, Phys. Rev. B **82**, 144522 (2010).

[27] P. Dai, J. Hu, and E. Dagotto, Magnetism and its microscopic origin in iron-based high-temperature superconductors, Nat. Phys. **8**, 709 (2012).

[28] T. Bayaraa, C. Xu, Y. Yang, H. Xiang, and L. Bellaiche, Magnetic-domain-wall-induced electrical polarization in rare-earth iron garnet systems: A first-principles study, Phys. Rev. Lett. **125**, 067602 (2020).

[29] J. Zhang, X. Shen, Y. Wang, C. Ji, Y. Zhou, J. Wang, F. Huang, and X. Lu, Design of two-dimensional multiferroics with direct polarization-magnetization coupling, Phys. Rev. Lett. **125**, 017601 (2020).

[30] I. Solovyev, R. Ono, and S. Nikolaev, Magnetically induced polarization in centrosymmetric bonds, Phys. Rev. Lett. **127**, 187601 (2021).

[31] J. Zhang, Y. Zhou, F. Wang, X. Shen, J. Wang, and X. Lu, Coexistence and coupling of spin-induced ferroelectricity and ferromagnetism in perovskites, Phys. Rev. Lett. **129**, 117603 (2022).

[32] A. Singer, S. K. K. Patel, V. Uhlíř, R. Kukreja, A. Ulvestad, E. M. Dufresne, A. R. Sandy, E. E. Fullerton, and O. G. Shpyrko, Phase coexistence and pinning of charge density waves by interfaces in chromium, Phys. Rev. B **94**, 174110 (2016).

[33] Y. Hu, T. Zhang, D. Zhao, C. Chen, S. Ding, W. Yang, X. Wang, C. Li, H. Wang, D. Feng, and T. Zhang, Real-space observation of incommensurate spin density wave and coexisting charge density wave on Cr (001) surface, Nat. Commun. **13**, 445 (2022).

[34] P.-J. Hsu, J. Kügel, J. Kemmer, F. Parisen Toldin, T. Mauerer, M. Vogt, F. Assaad, and M. Bode, Coexistence of charge and ferromagnetic order in fcc Fe, Nat. Commun. **7**, 10949 (2016).

[35] D. Qian, X. F. Jin, J. Barthel, M. Klaua, and J. Kirschner, Spin-density wave in ultrathin Fe films on Cu(100), Phys. Rev. Lett. **87**, 227204 (2001).

[36] A. Kubetzka, P. Ferriani, M. Bode, S. Heinze, G. Bihlmayer, K. von Bergmann, O. Pietzsch, S. Blügel, and R. Wiesendanger, Revealing antiferromagnetic order of the Fe monolayer on W(001): Spin-polarized scanning tunneling microscopy and first-principles calculations, Phys. Rev. Lett. **94**, 087204 (2005).

[37] S. Meckler, N. Mikuszeit, A. Preßler, E. Y. Vedmedenko, O. Pietzsch, and R. Wiesendanger, Real-space observation of a right-rotating inhomogeneous cycloidal spin spiral by spin-polarized scanning tunneling microscopy in a triple axes vector magnet, Phys. Rev. Lett. **103**, 157201 (2009).

[38] N. Romming, C. Hanneken, M. Menzel, J. E. Bickel, B. Wolter, K. von Bergmann, A. Kubetzka, and R. Wiesendanger, Writing and deleting single magnetic skyrmions, Science **341**, 636 (2013).

[39] E. A. Stepanov, V. Harkov, M. Rösner, A. I. Lichtenstein, M. I. Katsnelson, and A. N. Rudenko, Coexisting charge density wave and ferromagnetic instabilities in monolayer InSe, npj Comput. Mater. **8**, 118 (2022).

[40] F. Galli, R. Feyerherm, R. W. A. Hendrikx, E. Dudzik, G. J. Nieuwenhuys, S. Ramakrishnan, S. Brown, S. v. Smaalen, and J. Mydosh, Coexistence of charge density wave and antiferromagnetism in $Er_5Ir_4Si_{10}$, J. Phys.: Condens. Matter **14**, 5067 (2002).

[41] N. Hanasaki, S. Shimomura, K. Mikami, Y. Nogami, H. Nakao, and H. Onodera, Interplay between charge density wave and antiferromagnetic order in $GdNiC_2$, Phys. Rev. B **95**, 085103 (2017).

[42] D. Salamatin, V. Sidorov, S. Kichanov, A. Velichkov, A. Salamatin, L. Fomicheva, D. Kozlenko, A. Nikolaev, D. Menzel, M. Budzynski, and A. Tsvyashchenko, Coexistence of charge density wave and incommensurate antiferromagnetism in the cubic phase of $DyGe_{2.85}$ synthesised under high pressure, J. Alloys Compd. **755**, 10 (2018).

[43] M. A. Cazalilla, A. F. Ho, and M. Ueda, Ultracold gases of ytterbium: Ferromagnetism and Mott states in an SU(6) Fermi system, New J. Phys. **11**, 103033 (2009).

[44] M. A. Cazalilla and A. M. Rey, Ultracold Fermi gases with emergent SU(N) symmetry, Rep. Prog. Phys. **77**, 124401 (2014).

[45] C.-H. Huang, Y. Takasu, Y. Takahashi, and M. A. Cazalilla, Suppression and control of prethermalization in multicomponent Fermi gases following a quantum quench, Phys. Rev. A **101**, 053620 (2020).

[46] C.-H. Huang, M. Tezuka, and M. A. Cazalilla, Topological Lifshitz transitions, orbital currents, and interactions in low-dimensional Fermi gases in synthetic gauge fields, New J. Phys. **24**, 033043 (2022).

[47] C. N. Yang and S. C. Zhang, SO(4) symmetry in a Hubbard model, Mod. Phys. Lett. B **04**, 759 (1990).

[48] L. Wang, Y.-H. Liu, M. Iazzi, M. Troyer, and G. Harcos, Split orthogonal group: A guiding principle for sign-problem-free fermionic simulations, Phys. Rev. Lett. **115**, 250601 (2015).

[49] K. L. Lee, K. Bouadim, G. G. Batrouni, F. Hébert, R. T. Scalettar, C. Miniatura, and B. Grémaud, Attractive Hubbard model on a honeycomb lattice: Quantum Monte Carlo study, Phys. Rev. B **80**, 245118 (2009).

[50] S.-Y. Miyatake, K. Inaba, and S.-I. Suga, Three-component fermionic atoms with repulsive interaction in optical lattices, Phys. Rev. A **81**, 021603(R) (2010).

[51] K. Inaba and S. Suga, Superfluid, staggered state, and Mott insulator of repulsively interacting three-component fermionic atoms in optical lattices, Mod. Phys. Lett. B **27**, 1330008 (2013).

[52] H. Yanatori and A. Koga, Finite-temperature phase transitions in the SU(N) Hubbard model, Phys. Rev. B **94**, 041110(R) (2016).

[53] H. Yanatori and A. Koga, Finite temperature properties of three-component fermion systems in optical lattice, J. Phys. Soc. Jpn. **85**, 014002 (2016).

[54] R. A. Fontenele, N. C. Costa, R. R. dos Santos, and T. Paiva, Two-dimensional attractive Hubbard model and the BCS-BEC crossover, Phys. Rev. B **105**, 184502 (2022).

[55] Z. Zhou, Z. Cai, C. Wu, and Y. Wang, Quantum Monte Carlo simulations of thermodynamic properties of SU(2N) ultracold fermions in optical lattices, Phys. Rev. B **90**, 235139 (2014).

[56] Z. Zhou, D. Wang, Z. Y. Meng, Y. Wang, and C. Wu, Mott insulating states and quantum phase transitions of correlated SU(2N) Dirac fermions, Phys. Rev. B **93**, 245157 (2016).

[57] Z. Zhou, D. Wang, C. Wu, and Y. Wang, Finite-temperature valence-bond-solid transitions and thermodynamic properties of interacting SU(2N) Dirac fermions, Phys. Rev. B **95**, 085128 (2017).

[58] Z. Zhou, C. Wu, and Y. Wang, Mott transition in the π-flux SU(4) Hubbard model on a square lattice, Phys. Rev. B **97**, 195122 (2018).

[59] H. Georgi, *Lie Algebras in Particle Physics: From Isospin to Unified Theories* (Taylor & Francis, London, 2000).

[60] Y.-H. Liu and L. Wang, Quantum Monte Carlo study of mass-imbalanced Hubbard models, Phys. Rev. B **92**, 235129 (2015).

[61] D. Wang, Y. Li, Z. Cai, Z. Zhou, Y. Wang, and C. Wu, Competing orders in the 2D half-filled SU(2N) Hubbard model through the pinning-field quantum monte carlo simulations, Phys. Rev. Lett. **112**, 156403 (2014).

[62] E. Ibarra-García-Padilla, C. Feng, G. Pasqualetti, S. Fölling, R. T. Scalettar, E. Khatami, and K. R. A. Hazzard, Metal-insulator transition and magnetism of SU(3) fermions in the square lattice, Phys. Rev. A **108**, 053312 (2023).